



ELSEVIER

Physica B 304 (2001) 267–275

PHYSICA B

www.elsevier.com/locate/physb

Investigation on self-aligned HgTe nano-crystals induced by controlled precipitation in PbTe–HgTe quasi-binary compound semiconductor alloys

Manjong Lee, Choong-Un Kim*

Materials Science and Engineering Program, The University of Texas at Arlington, P.O. Box 19031, Arlington, TX 76019, USA

Received 3 May 2000

Abstract

The present paper reports the results of the controlled precipitation for the HgTe nano-crystals in the PbTe semiconductor matrix and demonstrates its effectiveness in producing well-organized and crystallographically aligned semiconductor nano-crystals. Following the same procedure used in metallic alloys, the semiconductor alloys are treated at 600°C for 48 h, quenched and aged up to 400 h at 300°C and 400°C to induce homogeneous nucleation and growth of HgTe precipitates. Examination of the resulting precipitates using transmission electron microscopy (TEM) reveals that the coherent HgTe precipitates form as thin disks along the {100} habit planes of PbTe matrix. It is also found that the precipitate undergoes a gradual shape change without any noticeable coarsening, from a disk to a cube, as the aging time increases. The microstructure after full aging is found to contain almost equal sized HgTe cubes, roughly 7 nm, that maintain coherency with {100} planes of the matrix. These results combined with the extreme dimension of the precipitates and the simplicity of the formation process leads to a belief that controlled precipitation can be an effective method in preparing a desirable quantum-dot microstructure. © 2001 Elsevier Science B.V. All rights reserved.

PACS: 67.80; 81.20.F; 81.30.M

Keywords: PbTe–HgTe; Coherent precipitates; Controlled precipitation; Quantum dots

1. Introduction

The realization of a dense array of semiconductor nano-crystals is a subject of extensive research in quantum-dot technology as quantum dots have unique physical properties related to its size-effects, for example, quantum confinement [1,2].

While the fundamental understanding of the quantum effect has been significant for a single quantum dot [3] or double quantum dots [4], its application to practical devices, where multiple quantum structures are essential, has been achieved on a limited scale. Several novel techniques have been developed in the past few years for creating multiple quantum dots in a glass or a polymer matrix [5–7]. However, the fabrication of nano-crystals in a semiconducting matrix phase

*Corresponding author. Fax: 1-817-272-2538.

E-mail address: choongun@uta.edu (C.-U. Kim).

has proven to be a challenging task. They traditionally rely on epitaxial film growth followed by patterning of the dots using lithography and on the self-assembly process of the epilayer [8–11]. Although these techniques enable the formation of a nearly perfect interface between the dot and the barrier matrix, the complexity of the process as well as its applicability only to thin film devices poses considerable limitations. Therefore, we introduce, in this study, controlled precipitation induced in compound semiconductor alloys as a simple and effective fabrication technique of the multiple quantum-dot (MQD) structure.

The concept of controlled precipitation of nano-crystals has much in common with that of the age hardening process routinely found in metal alloy [12,13]. It essentially consists of three heat treatments—solid solution thermal treatment, quenching and aging—conducted on an alloy system having a considerable solubility difference of alloying element with temperature. The solid solution treatment of the alloy produces a supersaturated solid solution. By quenching to room temperature, precipitation in the supersaturated alloy is suppressed. Finally, the alloy is aged at a temperature where controlled homogeneous nucleation and growth of precipitates occur. Due to slow diffusion kinetics at the aging temperature, the resulting precipitates can be extremely small and densely populated. When the size of the precipitate is sufficiently small, usually a few nanometers, it often shows lattice-coherency with the matrix, which is essentially the same interface as the one found in epilayers. Controlled precipitation should be equally effective for any type of alloy system, including semiconductor, in producing coherent nano-precipitates as long as the proper alloy system, composition, and heat treatment conditions are chosen.

The HgTe–PbTe quasi-binary system is chosen for our initial investigation from the possible semiconductor alloys where the effectiveness of controlled precipitation could be tested. As shown in Fig. 1, where the available phase diagram [14] of the system is shown, HgTe shows a considerable change in solid solubility with temperature. The maximum solubility of HgTe in PbTe at the

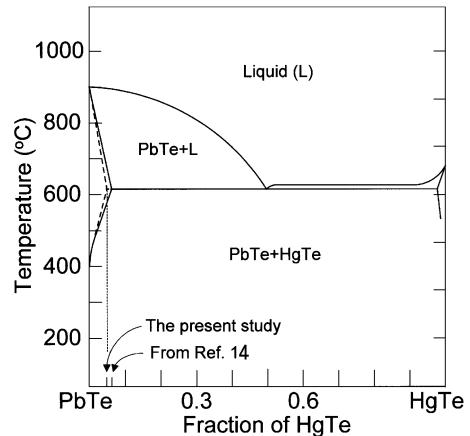


Fig. 1. A graphical representation of quasi-binary PbTe–HgTe phase diagram reproduced from Ref. [14]. The solvus line at the PbTe-rich end of phase diagram, which is newly determined by our investigation, is presented as a dotted line.

eutectic temperature ($605 \pm 5^\circ\text{C}$) is ~ 5 mol%, while the solubility becomes negligible at a temperature below 400°C . Also, PbTe shows negligible solubility in solid HgTe at nearly all temperatures. Furthermore, because the mutual solubility between HgTe and PbTe is almost negligible below 400°C , nearly pure HgTe precipitates in the pure PbTe matrix are expected. The PbTe bulk alloy containing 4 mol% HgTe (PbTe–4HgTe) is chosen in this study not only because it enables the use of controlled precipitation to produce HgTe quantum dots ($E_g = \sim 0$ eV at 300 K) in PbTe matrix ($E_g = \sim 0.3$ eV at 300 K) but also because it may have an immediate application such as thermoelectric devices [15–17] and infrared detectors [18].

This paper presents microstructural observations made in PbTe–4HgTe alloys which demonstrate the effectiveness of the controlled precipitation technique in producing a dense array of well-aligned nano-crystals with coherent interfaces. Unlike precipitates in metallic alloys, the HgTe precipitates show excellent thermal stability and resist coarsening. The mechanism behind such thermal stability is discussed in conjunction with the unique morphological evolution of precipitates found in this investigation.

2. Experimental procedures

The starting polycrystalline stoichiometric compounds, PbTe and HgTe, are synthesized by direct melting of the constituent elements, Pb, Hg and Te (purity higher than 99.999) in a sealed quartz ampoule filled with argon gas. To prevent any possible contamination during preparation, the quartz ampoules are carefully cleaned using nitric acid, hydrochloric acid, acetone, and de-ionized water, and finally coated with carbon [19]. The nominal size of the sealed ampoule is kept to a minimum, usually 15 mm in diameter and less than 10 cm long, to reduce the evaporative loss of the volatile constituents during melting. The back-fill argon gas is introduced only after a vacuum level of 10^{-6} Torr is achieved. The formation of PbTe and HgTe is confirmed using X-ray powder diffraction.

The PbTe–4HgTe alloy is prepared using the same procedure introduced above. The properly weighed HgTe and PbTe mixture, placed in a sealed quartz ampoule, is heated to 1000°C, 60°C above the melting temperature of PbTe, where the ampoule is subjected to a slight mechanical vibration for 30 min for complete melting. The melt is then slowly cooled to 600°C at 1°/min, then cooled to room temperature rapidly to minimize precipitation during cooling. The melt is then held at 600°C for 48 h to make supersaturated alloys. It is found that air cooling, achieved by exposing the ampoule to circulating air, is sufficient as a quenching treatment. At this stage, the grain size of the supersaturated polycrystalline solid solution of PbTe–4HgTe is a few mm. For the aging treatment, the alloy is sliced into several pieces, which are placed in individual sealed quartz ampoules. Aging treatments are carried out at two different temperatures, 300–400°C, for various time periods up to 500 h.

The equilibrium PbTe phase [20] has a NaCl structure with a lattice constant of 6.462 Å, while HgTe phase [21] has a sphalerite structure with a lattice constant of 6.453 Å. To characterize the constituent phases, X-ray diffraction methods, powder and double crystal diffraction, are also attempted. However, the resulting main X-ray peaks from these two crystals overlap within a

resolution limit, making them nearly impossible to separate for phase identification due to the close proximity of the lattice constants and crystal structure of the two constituent phases. Thus, transmission electron microscopy (TEM) is the primary technique used in this investigation for the characterization of the microstructural evolution of the alloy. TEM sample preparation requires special attention. Our preliminary investigation indicates that the precipitation behavior changes drastically when the alloy is stored too long as a thin foil, especially when it is stored under vacuum. For this reason, TEM samples are made with minimum exposure to vacuum and heat. Properly cut ingots are bonded to copper grids, mechanically ground to form a dimple and then briefly ion milled. TEM characterization is conducted immediately after the sample preparation.

3. Results

3.1. Precipitation of HgTe in PbTe–4HgTe

Examination of the alloys after the quenching treatment reveals that the air-cooling used in this study successfully suppresses the formation of HgTe precipitates because no indication of precipitates is found in the as-quenched alloys. The air-cooling method usually takes 10 min to accomplish the complete cooling of the alloys. Although not substantiated, a slower cooling rate than this may also be used as a quenching method, adding considerable flexibility of the controlled precipitate method in real application. It is also found that the as-quenched alloys have a well-ordered crystal structure of PbTe solid solution with a very low concentration of dislocations and other types of crystal defects.

The aging treatment of the alloy at 300–400°C produces a large population of HgTe precipitates of extremely small size. The shape of initial precipitates is found to be a plate with a diameter slightly larger than 10 nm and a few nm thick, the face of which is aligned with {100} planes of the PbTe matrix. Fig. 2 presents a set of TEM micrographs taken from the sample aged at 400°C for 25 h. These micrographs show TEM

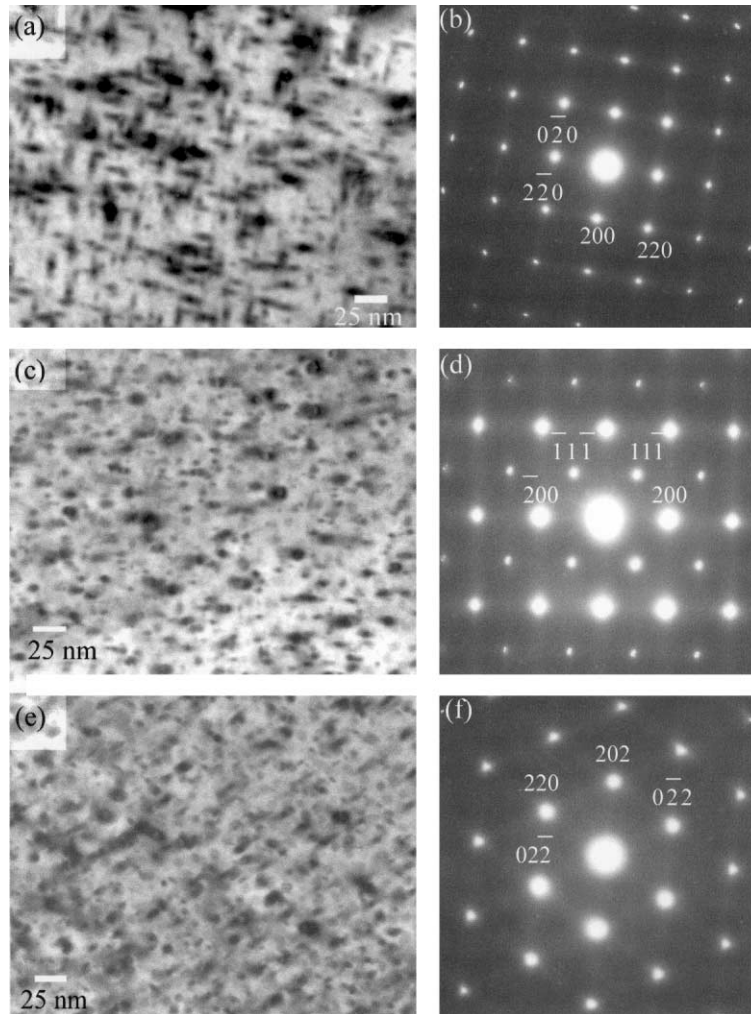


Fig. 2. TEM micrographs (bright field image and diffraction pattern) showing the formation of HgTe precipitates after 25 h aging at 400°C taken at three different zone axes: (a), (b) $\langle 100 \rangle$; (c), (d) $\langle 110 \rangle$; (e), (f) $\langle 111 \rangle$.

bright field images of the HgTe precipitates and corresponding electron diffraction patterns (DP) taken at three different zone axes, $\langle 100 \rangle$, $\langle 110 \rangle$ and $\langle 111 \rangle$. It can be seen that the alloy contains an extremely high density of precipitates, which is estimated to be more than $30,000/\mu\text{m}^3$. The exact size and size distribution of the precipitates is rather difficult to determine because the strain field around precipitates often obscures the exact location of the phase boundary. A careful examination of the precipitates in various samples

and multiple beam directions, however, suggest that the precipitate size is quite uniform at least within the resolution of our measurement.

The diffraction pattern in Fig. 2b clearly shows the presence of thin plates along $\{100\}$ habit planes. The HgTe plates are too small to produce their own diffraction spots, yet their presence along $\{100\}$ habit planes produces streaks around (200) spots from the matrix. From the changes of the precipitate image as well as the streak directionality with beam direction, it is concluded

that the precipitate is a thin disk. Of the three sets of plates aligned with each $\{100\}$ PbTe plane, only two sets of plates are visible in the image taken at $\langle 100 \rangle$ direction (Fig. 2a). The invisible precipitates in this case are the plates whose face is perpendicular to the beam direction. The precipitate is very thin in this direction, resulting in an insignificant amount of contrast. It can be seen that the precipitate image progressively evolves from needle-like to circular as the beam direction changes from $\langle 100 \rangle$ to $\langle 111 \rangle$. This type of image change with beam direction is possible only when the precipitate is a thin disk with $\{100\}$ habit planes. Notice also that the $\langle 110 \rangle$ diffraction pattern contains super-lattice spots (weaker intensity). The presence of the super-lattice diffraction spots is a strong indication that the PbTe matrix maintains its ordered crystal structure during precipitation [22].

The HgTe precipitates shown in Fig. 2 are coherent precipitates, meaning that the lattice is continuous across the matrix-precipitate interface. This is evidenced by the presence of lattice strain around the precipitates. The lattice constant of HgTe is slightly larger than that of PbTe. In order to maintain the lattice continuity, either expansion of the PbTe lattice or contraction of the HgTe lattice should occur. Since the stiffness of HgTe is much higher than that of PbTe [23], most of the lattice distortion is likely to be generated within the PbTe matrix near the face of the HgTe plate. The strain field from the lattice distortion in the PbTe matrix is most pronounced along the $\langle 110 \rangle$ and $\langle 111 \rangle$ directions, ending within a few nm of the face of the HgTe precipitates. An example of a strain field in the PbTe matrix is shown in the bright field image of precipitates (Fig. 3) aged at 400°C for 25 h taken from a $\langle 112 \rangle$ beam direction. As indicated in the micrograph, the contrast lobe of strain fields with a zero contrast line perpendicular to the two g vectors, $g_{\langle 110 \rangle}$ and $g_{\langle 111 \rangle}$, can be seen [24]. The presence of such a unique contrast is a result of a strain field existing in the $\langle 110 \rangle$ and $\langle 111 \rangle$ directions. Also, notice the shape of the strain field lobe, which means that the precipitate itself takes a rounded shape [24]. The $\{100\}$ habit plane for precipitation and the existence of interface coher-

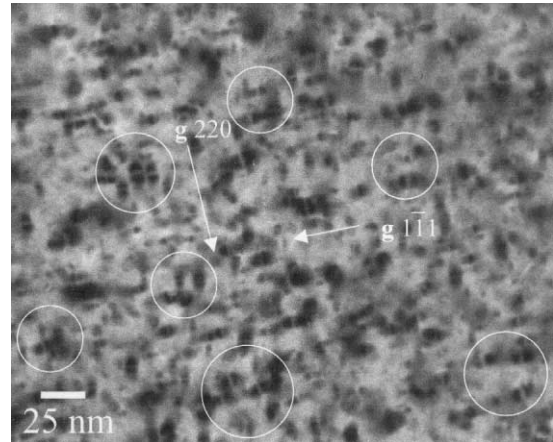


Fig. 3. TEM micrograph showing the $\langle 112 \rangle$ zone axis microstructure of the alloy after 25 h aged at 400°C . Notice the absence of the contrast normal to $g_{\langle 110 \rangle}$ and $g_{\langle 111 \rangle}$.

ency suggest that the HgTe precipitation is achieved by aligning $\{100\}$ planes of the HgTe micro-crystals with $\{100\}$ planes of the PbTe matrix, i.e. $\{100\}_{\text{HgTe}} \parallel \{100\}_{\text{PbTe}}$ and $[100]_{\text{HgTe}} \parallel [100]_{\text{PbTe}}$.

The examination of precipitates in the alloys aged at 300°C shows basically the same characteristics as those found in the alloys aged at 400°C . In contrast to our expectation, the size and population of the precipitates is not greatly affected by the aging temperatures, at least within the experimental conditions used in this investigation. The aging temperature, however, does influence the kinetics of the precipitate-shape evolution as discussed in detail in the following section.

3.2. Evolution of precipitate shape with aging

To investigate the thermal aging effect on the shape change of the HgTe precipitate, the alloys are aged for up to 500 h at two different aging temperatures, 300°C and 400°C . In a typical metallic alloy, the precipitate coarsens with further aging once precipitation is complete. During coarsening, the size of the precipitates increases while their number decreases. However, the HgTe precipitates do not seem to follow the normal coarsening process. Figs. 4 and 5 illustrate the evolution of precipitate image with aging time at

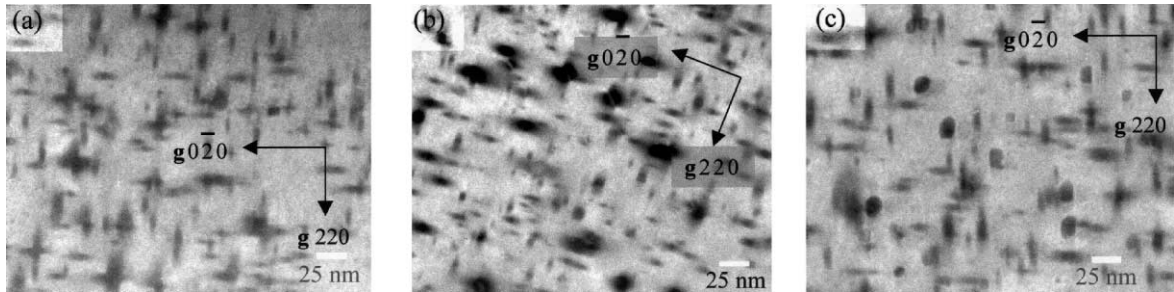


Fig. 4. TEM micrographs showing the evolution of precipitation aged at 300°C as a function of aging time: (a) 5 h, (b) 125 h, and (c) 400 h.

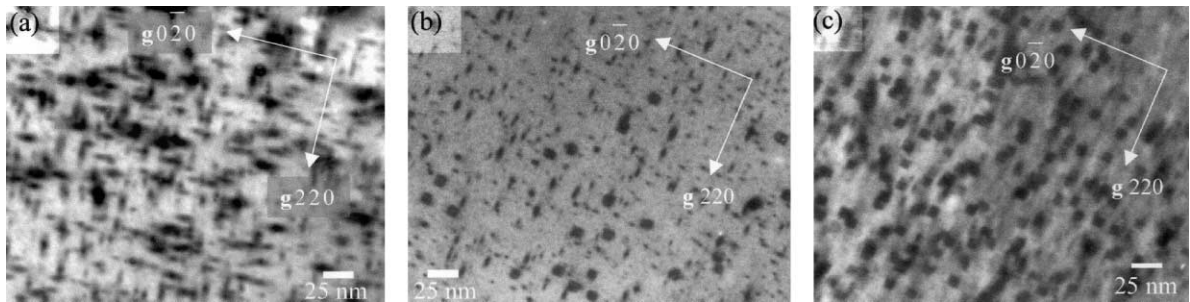


Fig. 5. TEM micrographs showing the evolution of precipitation aged at 400°C as a function of aging time: (a) 25 h, (b) 125 h, and (c) 300 h.

300°C and 400°C, respectively. It can be seen that, in both cases, the precipitate density is not significantly changed with aging time. The insignificant density change makes it difficult to determine the completion time of the precipitation process. However, TEM examinations of the precipitate after a short aging treatment, 1–5 h, reveals that the precipitation is probably complete within a few hours.

While the density of precipitates appears to be constant, their shape and size evolve with aging time. As the aging time increases, the precipitate, initially disk-shaped, starts to develop facets and ultimately evolves into a cube. The faceted nature of the precipitate is clearly visible in the sample aged for 400 h at 300°C (Fig. 4b). Fully developed precipitates are shown in Fig. 5c, where they are visible as squares. Based on observation from several directions, these squares are determined to be cube faces. Each cube face is aligned with the $\{100\}$ planes and $\langle 100 \rangle$ directions of PbTe matrix. It is also noted that the length of the

cube edge is smaller than the diameter of the initial disk. The measured length of the cube-edge is, on average, 7 nm, which is considerably smaller than the initial diameter of the disk. These results, the insignificant variation of precipitate density and the development of a cube with a smaller edge size, suggest that the coarsening of HgTe does not proceed between precipitates but by redistribution of HgTe molecules within a single precipitate in order to promote the formation of the cube. If true, the total volume of each precipitate should be maintained irrespective of the aging time. The best estimate of the initial disk dimension is roughly 12 nm in diameter and 4 nm in thickness, making its total volume, $450 \mu\text{m}^3$, assuming a perfect cylindrical shape. The volume of the cube is 7^3 (343) μm^3 . Considering that the thickness of a precipitate is usually smaller at the edge of a disk, it is plausible that volume is preserved.

Fig. 6 summarizes the evolution of precipitates as established in this study, presenting the sche-

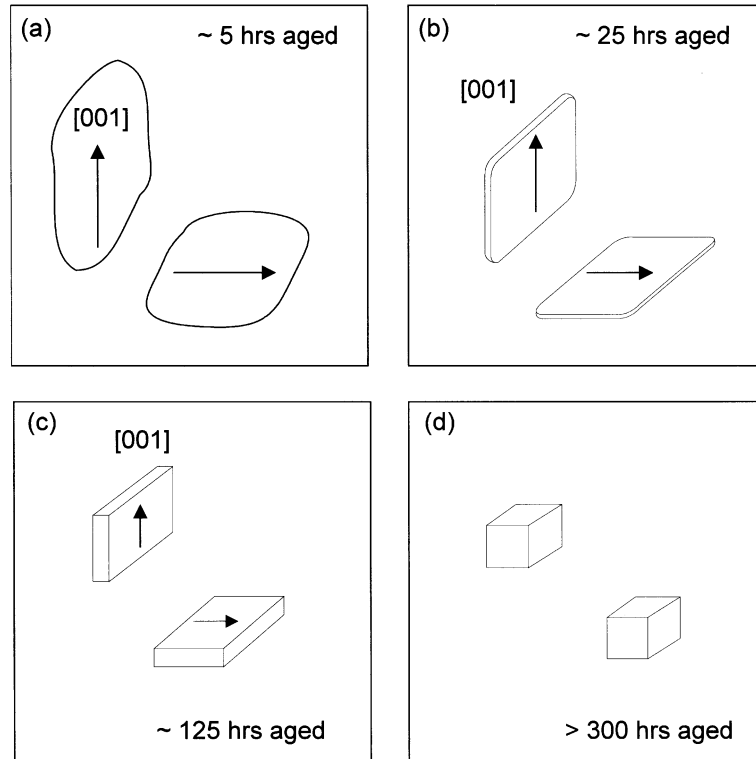


Fig. 6. A schematic diagram showing the evolution of the precipitate shape as a function of aging time found in this investigation. For simplicity, two sets of precipitates among three are drawn in this diagram.

matics of the precipitate shape and size as a function of aging time. Different aging temperatures simply change the kinetics of the process illustrated here. As indicated in this figure, the precipitation of HgTe is initiated by the formation of a thin disk along the $\{100\}$ planes of the PbTe matrix. As aging progresses, the precipitate grows in thickness by taking HgTe molecules from its edge. At this stage, a faint yet identifiable image of the disk starts to appear in TEM images due to an enhanced contrast caused by the increased thickness. The gradual shrinkage of the disk diameter together with growth normal to the disk face eventually leads to the formation of the cube. The formation of a cube appears to enhance the size uniformity of the precipitate (Fig. 5c). This precipitate evolution process also reduces lattice strain without destroying interface coherency.

4. Discussion

The precipitation mechanism in the PbTe–4HgTe alloy system shares some similarities with the one usually found in metallic alloys. The formation of crystallographically aligned coherent precipitates during the controlled precipitation is common in metallic alloys, a well-known example of which is GP (Guinier–Preston) zones. The precipitation in PbTe–4HgTe should form following a similar nucleation process. The homogeneous nucleation proceeds by collecting Hg atoms or HgTe molecules within their effective diffusion distance. Through the periodic perturbation of the HgTe concentration, nucleation ensues on a habit plane of the lowest interface and strain energy. The precipitate resulting from this process is usually a thin disk if the habit plane is $\{100\}$. As diffusion is involved in the precipitation process, the size and

spacing uniformity depend on the crystal quality of the matrix. If the matrix is free from crystal defects that provide easier diffusion paths, all precipitates will have the same size and inter-spacing. Matrix quality is believed to be excellent because no significant crystal defects including dislocations are detected in the TEM study of aged PbTe samples, leading to the conclusion that the PbTe matrix is well annealed and likely to have a low concentration of dislocations. Therefore, the size and spacing uniformity of HgTe precipitates are believed to be excellent. This belief is at least partially supported by the size analysis of the cube precipitates shown in Fig. 5c.

The HgTe precipitation observed in this study is quite unique and demands further investigation. Although the precipitation mechanism appears to be similar to the ones found in others systems, there is one particular factor that is strikingly different from the others. It is the evolution of the HgTe precipitate shape during aging process. It is found that the HgTe precipitate progressively changes its shape from a disk to a cube without any apparent indication of coarsening. The shape change itself is not a new finding and is known to occur in various metallic alloy systems. For example, Ni₃Al precipitates in Ni–Al alloys can change their shape from spheres or cubes to disks [25,26]. Studies on the shape change suggest that it is a result of the interplay between the interface energy (surface and strain energy) and the precipitate size. The precipitate takes shape in a direction to minimize the total interface energy. As the relative contribution of the surface energy and the strain energy depends on the size of the precipitate, the preferred shape of a precipitate can change as the precipitate undergoes coarsening. In case of Ni₃Al, for example, the preferred shape at precipitation stage is either a cube or a sphere because the surface energy is a predominant factor in determining the total interface energy. As the precipitate coarsens, the strain energy becomes more predominant, which eventually promotes shape change to a disk. The mechanism of shape change in HgTe is not straightforward like Ni₃Al mainly because the change occurs without any apparent precipitate coarsening. Although some degree of coarsening should occur, its insignificant

extent, if any, cannot explain the apparent change in the shape. According to the observed shape change, the interface energy of HgTe precipitate is initially determined by the strain energy and later by the surface energy. As the precipitate size remains similar during aging the process, such an energy change is induced by the size. A more plausible explanation is the relaxation of strain energy by the reconfiguration of HgTe internal structure during aging and thereby promotion of a shape controlled by surface energy. While several mechanisms of stress relaxation, such as vacancy generation/destruction and the order–disorder phase transformation of HgTe phase can be suggested, the exact mechanism remains as future work.

Although several aspects of observations need further investigation, this study clearly demonstrates the effectiveness of controlled precipitation in achieving a semiconductor microstructure in which a dense array of coherent nano-crystals is dispersed with a fine regularity along a specific orientation of the matrix. Its application to practical devices, either in bulk or thin film forms, would certainly extend the area where QD phenomena can be useful. In particular, the method could be extremely useful when the devices require the use of bulk materials rather than the conventional thin film, for example, thermoelectric and some optical devices. Undoubtedly, there are numerous issues to be resolved before this technique can be applied to real devices, including the control of precipitate size and quantum effect associated with precipitates. These issues, along with the details of the mechanism of precipitation in semiconductor alloys, are currently under investigation in this laboratory.

5. Conclusions

The controlled precipitation performed on the PbTe–4HgTe semiconductor alloy reveals that HgTe precipitation initially takes place as a thin disk along the {100} habit plane of the PbTe matrix. While the exact mechanism is not clear, two aging temperatures produce disk-shaped precipitates that are almost equal in size, 12 nm in

diameter and 4 nm thick, with a density over $30,000/\mu\text{m}^3$. Further aging does not cause considerable coarsening of these precipitates. It instead results in a reconfiguration of the precipitate shape, from a disk to a cube (~ 7 nm in edge), probably due to interplay between the elastic energy and the surface energy caused by internal reconfiguration in HgTe precipitate. These results, the first of its kind, mean that controlled precipitation can be developed into an effective and simple way of producing nano-scale semiconductor crystals which are self-aligned and organized.

Acknowledgements

This work is supported by the Research Enhancement Program at the University of Texas at Arlington (UTA). The materials characterization center at UTA also provided the characterization equipment used in this study. The authors wish to express their sincere gratitude to Drs. Magnusson, Kirk, Nolas and Elsenbaumer for providing encouragement and useful insights.

References

- [1] A. Tackeuchi, S. Muto, *Mater. Sci. Eng. R22* (1998) 79.
- [2] S.Y. Ren, *Solid State Commun.* 102 (1997) 479.
- [3] D. Gammon, E.S. Snow, D.S. Katzer, *Appl. Phys. Lett.* 67 (1995) 2391.
- [4] C.H. Crouch, C. Livermore, R.M. Westervelt, *Appl. Phys. Lett.* 71 (1997) 817.
- [5] A. Demourgues, G.N. Greaves, R. Bilborrow, G. Baker, A. Sery, A.J. Dent, B. Speit, *Physica B* 208–209 (1995) 354.
- [6] B.L. Justus, R.J. Tonucci, A.D. Berry, *Appl. Phys. Lett.* 61 (1992) 3151.
- [7] D. Cotter, H.P. Girdlestone, K. Moulding, *Appl. Phys. Lett.* 58 (1991) 1455.
- [8] M.A. Reed, J.N. Randall, R.J. Aggarwal, R.J. Matyi, T.M. Moore, A.E. Wetsel, *Phys. Rev. Lett.* 60 (1988) 535.
- [9] T. Fukui, S. Ando, Y. Tokura, T. Toriyama, *Appl. Phys. Lett.* 58 (1991) 2018.
- [10] J.M. Moison, L. Leprince, F. Barthe, F. Houzay, N. Lebouche, J.M. Gerard, J.Y. Marzin, *Appl. Surf. Sci.* 92 (1996) 526.
- [11] D. Leonard, M. Krishnamurthy, C.M. Reaves, S.P. Denbaars, P.M. Petroff, *Appl. Phys. Lett.* 63 (1993) 3203.
- [12] R.B. Nicholson, G. Thomas, J. Nutting, *J. Inst. Met.* 87 (1958) 429.
- [13] J.W. Martin, in: *Precipitation Hardening*, Pergamon, New York, 1968.
- [14] V.G. Vanyarkho, V.P. Zlomanov, A.V. Novoselova, *Izv. Akad. Nauk USSR, Neorg. Mater.* 6 (1970) 133.
- [15] T.C. Harman, P.J. Taylor, D.L. Spears, M.P. Walsh, Y.F. Chen, *J. Electron. Mater.* 29 (2000) L1.
- [16] T.C. Harman, D.L. Spears, M.P. Walsh, *J. Electron. Mater.* 28 (1999) L1.
- [17] H. Djerassi, J.H. Albany, G. Lesoult, G. Beauvais, *Proceedings of the Third International Conference on Thermoelectric Energy Conversion*, Arlington, TX, 1980, p. 217.
- [18] Y. Yukun, L. Wenming, Y. Lei, S. Xin, X. Lixing, H. Lantain, *Infrared Phys. Technol.* 38 (1997) 9.
- [19] Y.I. Ravich, B.A. Efimova, I.A. Smirnov, in: L.S. Stil'bans (Ed.), *Semiconducting Lead Chalcogenides*, Plenum, New York, 1970, pp. 15–26.
- [20] G. Nimtz, in: K. Hellwege, O. Madelung (Eds.), *Numerical Data and Functional Relationships in Science and Technology, Landolt-Börnstein, New Series Group III*, Vol. 17, Springer, Berlin, 1983, p. 170.
- [21] A. Werner, H.D. Hochheimer, K. Strössner, A. Jayaraman, *Phys. Rev. B* 28 (1983) 3330.
- [22] B.D. Cullity, in: *Element of X-ray Diffraction*, 2nd Edition, Addison-Wesley, Reading, MA, 1978, pp. 383–393.
- [23] L.I. Berger, in: *Semiconductor Materials*, CRC Press, New York, 1997, pp. 210–213.
- [24] D.B. Williams, C.B. Carter, in: *Transmission Electron Microscopy: A Textbook for Materials Science*, Plenum Press, New York, London, 1996, pp. 403–421.
- [25] A.G. Khachatryan, S.V. Semenovskaya, J.W. Morris Jr., *Acta Metall.* 36 (1988) 1563.
- [26] Y. Wang, A.G. Khachatryan, *Acta Metall. Mater.* 43 (1995) 1837.